Magazine of Civil Engineering

ISSN 2071-0305

journal homepage: http://engstroy.spbstu.ru/

DOI: 10.18720/MCE.94.3

The geogrid-reinforced gravel base pavement model

S.A. Matveev*, E.A. Martynov, N.N. Litvinov, G.M. Kadisov V.A. Utkin
Siberian State Automobile and Highway University, Omsk, Russia
** E–mail: dfsibadi@mail.ru*

Keywords: granular roadbed basis, geogrid reinforcement, stiffness, deflections, design model, multilayered plate

Abstract. The design model of reinforced crushed stone layer calculating as a multilayer plate on an elastic base using the technical theory of bending and the Bubnov-Galerkin method is proposed, which makes it possible to theoretically calculate and justify the effectiveness of using various types of geosynthetic materials for reinforcing pavement bases made of granular materials. The model is based on the hypothesis that the reinforced granular layer is deformed like a plate on an elastic base because of the mechanical connection with the geogrid. The calculating model is a multilayer plate consisting of an arbitrary number of solid homogeneous rigidly interconnected layers. The possibility of using this model for calculation of reinforced granular pavement base is confirmed experimentally. The results of the stamp tests showed satisfactory agreement with the results of theoretical studies. The discrepancy did not exceed 15 %.

1. Introduction

One of the main structural elements of flexible road pavement is a base of granular material – crushed stone or gravel. An effective way to increase the rigidity of such a base is to reinforce it with a geogrid or geocell material. This makes it possible to increase a load bearing capacity and the service life of the pavement. At the same time, research [1] shows that the reinforcement of road structures is economically advantageous, since the use of geogrids in the roads construction provides significant saving money.

Reinforcing geogrids are made of raw materials of various types: polymer and mineral. They have different dimensions and shape of the cell, that significantly affects the deformability of the reinforced layer, the mechanism of which is not fully understood. This is due to the lack of scientifically based, reliable, experimentally confirmed models of deformation of reinforced bases of granular material, and also of the theory of calculation of pavements with reinforced layers, including layers of granular material.

In paper [2] a one-dimensional mathematical model is proposed for modelling geosynthetic-reinforced granular fills over soft soils subject to a vertical surcharge load. The geosynthetic reinforcement consists of a membrane (geogrid, orgeotextile) placed horizontally in engineered granular fill, which is constructed over soft soil. The proposed model is mainly based on the assumption of a Pasternak shearlayer. The results of full-scale accelerated load testing [3] demonstrate the benefits of using geosynthetics in terms of reducing the permanent deformation in the pavement structure. The authors [4, 5] were able to develop elastic solutions for geogrid-stabilized base courses over subgrade by considering lateral restraint and tensioned membrane effects. The analytical solutions were then employed to estimate the reduction of vertical stresses underneath the geogrid compared with the measured results.

The results of full-scale laboratory tests on geogrid reinforcements in unpaved roadway sections are presented in papers [6, 7]. The test sections were instrumented to measure geosynthetic deformation and to get information about the development of permanent strains in the geogrid during traffic loading. In addition, this study was performed to evaluate the integrity and performance requirements for geogrid junctions. An attempt to identify mechanical and physical properties of geogrids was made in the study Tang [8]. In works [9, 10], the elastic stiffness of a geogrid and its tensile rupture strength at a different temperature regimes were investigated. An empirical model of geogrid deformations under cyclic loading was proposed in [11]. The interaction features of a soil with geogrid at different loading rates, also under shear at cyclic loading, were studied in [12–14].

Matveev, S.A., Martynov, E.A., Litvinov, N.N., Kadisov, G.M., Utkin, V.A., The geogrid-reinforced gravel base pavement model. Magazine of Civil Engineering. 2020. 94(2). Pp. 21–30. DOI: 10.18720/MCE.94.3

A presence of significant structural deformations is a characteristic feature of a granular medium deformation. Due to these deformations, the grains of the lower row of the deformable granular layer are embedded in the base soil. In this case, there is a mutual penetration of the material of one layer into another. Professor Shestakov set the depth of individual crushed stone grain indentation approximately corresponds to its characteristic transverse dimension. Thus, the actual thickness of the upper layer is reduced. In order to preserve the design thickness of the upper layer in the absence of reinforcement, it is necessary to overspend the stone material. The geogrid, located at the level of the granular layer bottom, performs not only the functions of reinforcement, but also the separation of layers. It prevents the penetration of grains of gravel in the underlying sand layer. This makes it possible to prevent overspending of the stone material, and even to save it.

Ferellec and McDowell [15] created a model of ballast–geogrid interaction using the discrete-element method, studying the working properties of reinforced and non-reinforced gravel cushion on soft subsoil.

The soil reinforcement method, which consists of placing a geogrid at the bottom of granular layer, increases the load transfer on the underlying base distribution on top of subgrade layer [16]. In accordance with Abu-Farsakh and Chen [17] the inclusion of geogrid base reinforcement results in redistributing the applied load to a wider area, thus reducing the stress concentration and achieving an improved vertical stress. Alexandrov [18] has come to a similar conclusion, arguing that the presence of a reinforcing layer inside the granular medium changes the angle of distribution of vertical stresses in it.

Geogrid reinforcement of granular base layers of flexible pavements was carried out at the end of 80-th at the University of Waterloo. Reinforcing materials are incorporated into the base layer of flexible pavements so that the two materials act together. In summary, for optimum grid reinforcement of flexible pavements, the grid must be placed in a zone of moderate elastic tensile strain (i.e., 0.05 to 0.2 percent) beneath the load center, and maximum permanent strain in the grid over the design life should not exceed 1 to 2 percent, depending on the rut depth failure criteria [19].

Existing methods for reinforced granular pavement bases calculation are based on traditional methods for calculating flexible road pavements developed several decades ago. The difference between existing methods of calculation reinforced and unreinforced structure is the introduction of additional amplification factor obtained empirically.

New approach to reinforced granular base of pavement calculation is based on the model of a reinforced granular layer deformation like a multi-layer plate on an elastic base. The theoretical principles for the reinforced road structure calculating as a multilayer plate on an elastic foundation were developed by Matveev and Nemirovsky, further developed in [20] and experimentally confirmed in [21, 22]. The hypothesis that the reinforced granular layer works as a plate on an elastic base is confirmed in these studies, as well as in the works of other authors. The granular layer is actually a discrete medium and does not perceive tensile stresses. In the part of the granular layer adjacent to the geogrid reinforced granular material behaves like a continuous medium due to mechanical engagement with the geogrid, as well as due to friction forces between the individual grains. The reinforcing effect is achieved by the joint functioning of the geogrid with a granular material. In this case the geogrid ribs perceive horizontal tensile forces arising at the level of the reinforcing interlayer. The influence zone of the geogrid placed inside the granular layer as a reinforcing interlayer is extended to 15 cm up or down from the plane of reinforcement [23]. In this zone the additional shear resistance of the granular material caused by reinforcement is decreased with increasing distance from the geogrid. This phenomenon was experimentally confirmed in paper [24], where it was noted that the granular layer reinforcement makes the pseudo-plate effect.

From the analysis of the above sources, it follows that the development of a design model of a reinforced granular base in the form of a model of an equivalent in rigidity of a multilayer plate on an elastic base is actual. Therefore, the purpose of this study is to create a design model allowing setting the effect of geogrid parameters on the stiffness of the reinforced granular base of the pavement.

The problems of this study are to describe the stiffness characteristics of each of the layers, taking into account the basic properties and characteristics of the material constituting each layer; to describe the stiffness characteristics of the whole package of layers; to select a suitable method for calculating the multilayer plate; to perform the experimental studies in the form of stamp tests of the base of pavement structure.

The novelty of this work lies in the fact that the results of experimental studies of a crushed stone base reinforced with a geogrid with steel wires were obtained for the first time. Previously, bases with this type of geogrid have not been tested. The theory for calculating of flexible pavements bases has been developed. This theory allows us to determine the coefficient of decrease in the elastic deflections of reinforced bases for different types of reinforcement.

The results of this study can find practical application in the calculation of flexible pavements.

2. Methods

2.1. Theoretical solution

The object of the study is the base of pavement structure shown in Figure 1a. The upper layer is the crushed stone layer with thickness h_1. The underlying soils are the sand with thickness of layer h_0. The reinforcement in the form of a geogrid is located on the boundary between the crushed stone and the sand layer.

The geogrid is formed from flat metal-plastic strips connected at an angle of 90° and superimposed one upon the other in height. The geogrid cell size is $L \times L$. Metal-plastic strips consist of a bearing part and a covering. The bearing part of the strips is steel fibers of spring wire with a diameter of 0.6 mm, located at a certain distance from each other without interweaving. The number of wires inside one strip can change from 3 to 9. In the experiment there were used geogrids with number of wires 3, 6 and 9 in one strip respectively. A covering of strips is low pressure polyethylene. The connection of metal-plastic strips between themselves is carried out by thermal welding methods. The geogrid scheme is shown in Figure 1b.

In order to determine the deflections of the geogrid-reinforced granular layer, let us accept a hypothesis that a crushed stone layer will behave as a solid connected medium, provided that a geogrid is located at the base of the layer, similar to that shown in Figure 1a.

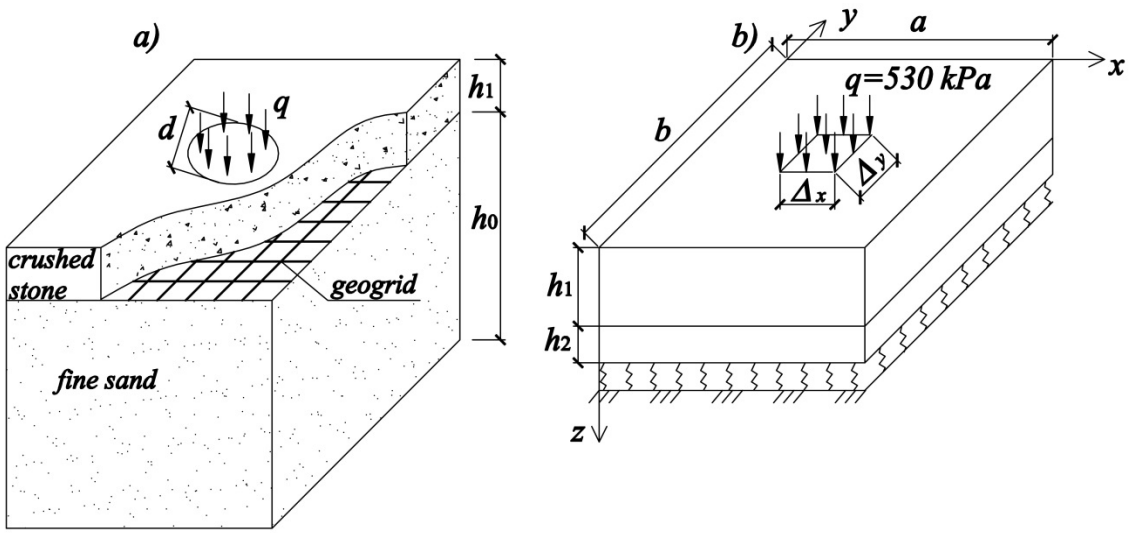

Figure 1. The reinforced base design: a) the base construction; b) the geogrid scheme.

A geogrid accepts tensile stresses and makes it possible to simulate a reinforced granular layer as plate on an elastic base [24]. In this case the technical theory of bending plate [20] can be used for reinforced granular base design. At small strains the internal forces in such plates arise from bending. In this case, both tensile and compressive stresses appear in the layer. Crushed stone as a discrete material is not able to perceive a tensile stresses. When reinforcing a crushed stone particle is caught by transverse ribs of a geogrid and cause tensile of the longitudinal ribs. It allows us to simulate a geogrid as a continuous composite layer or a thin plate with thickness h_2 (Figures 2, 3), working in tension. Such a plate does not have bending stiffness factor. But if it is included as an additional layer in the composition of the multi-layer plate, it will have a significant impact on the overall bending rigidity of the whole structure. In this way, the reinforced crushed stone layer can be simulated as a plate on an elastic base. The plate consists of two rigidly connected layers (Figure 2).

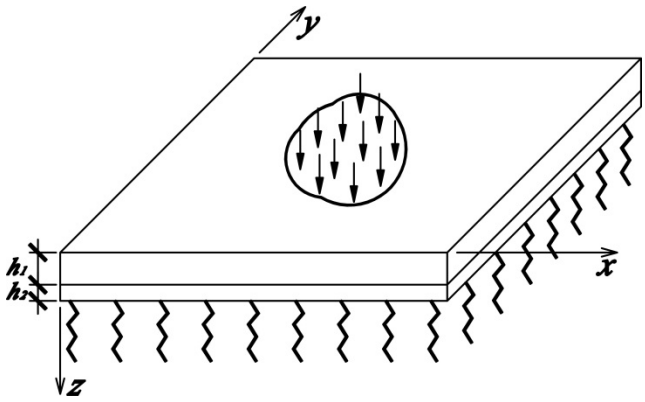

Figure 2. The model of two-layer plate located on an elastic base.

The physical and mechanical characteristics of layers will differ. Some layers of a multilayer plate may not work on bending, but they are formally included in the overall rigidity of the whole structure in accordance with the theory developed in the Siberian Branch of the Russian Academy of Sciences [2].

We accept the Kirchhoff-Love hypothesis, which will be valid for each layer of multilayer plate bending. The differential equation of bending plate is represented in the following form [20]:

$$D_{11}\frac{\partial^4 w}{\partial x^4}+3D_{13}\frac{\partial^4 w}{\partial x^3\partial y}+2\left(D_{12}+D_{33}\right)\frac{\partial^4 w}{\partial x^2\partial y^2}+ 2D_{23}\frac{\partial^4 w}{\partial x\partial y^3}+D_{22}\frac{\partial^4 w}{\partial y^4}+C_z w+q=0, \quad (1)$$

where C_z is the coefficient of soil reaction;

$q = q(x, y)$ is the intensity of the loads on the surface plate;

$w = w(x, y)$ is the deflection function;

$D_{11}...D_{33}$ are constants of the plate characterizing its elastic properties:

$$\begin{aligned} D_{11} &= d_{11}+c_{11}\cdot c_{11}^{*};\\ D_{12} &= A_{12}^{(1)}g_1+A_{12}^{(2)}g_2;\\ D_{22} &= A_{22}^{(1)}g_1+A_{22}^{(2)}g_2;\\ D_{33} &= A_{33}^{(1)}g_1+A_{33}^{(2)}g_2. \end{aligned} \quad (2)$$

Included the first Equation (2) constants d_{11}, C_{11}, c_{11}^{*} calculated by the formulas

$$\begin{aligned} d_{11} &= A_{11}^{(1)}g_1+A_{11}^{(2)}g_2;\\ c_{11}^{*} &= \frac{(c_{21}b_{12}-c_{11}b_{22})}{(b_{11}b_{22}-b_{12}b_{21})};\\ c_{11} &= A_{11}^{(1)}p_1+A_{11}^{(2)}p_2;\\ c_{21} &= A_{21}^{(1)}p_1+A_{21}^{(2)}p_2, \end{aligned} \quad (3)$$

where A_{kj} is the coefficient of proportionality between stress and strain accepted for the first (unreinforced) layer:

$$\begin{aligned} A_{11}^{(1)} &= A_{22}^{(1)}=\frac{E}{1-\nu^2};\\ A_{33}^{(1)} &= \frac{E}{2\left(1+\nu\right)};\\ A_{12}^{(1)} &= A_{21}^{(1)}=\frac{\nu E}{1-\nu^2}, \end{aligned} \quad (4)$$

Here E is the elasticity modulus of crushed stone layer;

ν is Poisson's ratio.

The constants included in the Equation (3) are determined by the formulas

$$g_1=\frac{h_1^3}{3};\quad g_2=\frac{1}{3}\left(3h_1^2+3h_1h_2+h_2^2\right)h_2, \quad (5)$$

$$p_1=\frac{h_1^2}{2};\quad p_2=\frac{1}{2}\left(2h_1+h_2\right)h_2, \quad (6)$$

here h_1, h_2 are thickness of the 1-st and 2-nd layers respectively;

$$b_{11} = A_{11}^{(1)} h_1 + A_{11}^{(2)} h_2;$$
$$b_{22} = A_{22}^{(1)} h_1 + A_{22}^{(2)} h_2; \quad (7)$$
$$b_{12} = A_{12}^{(1)} h_1 + A_{12}^{(2)} h_2.$$

The total cross-sectional area of the reinforcing fibers oriented along the x-axis, is

$$A_{ax} = n_x \ A_f, \quad (8)$$

where A_f is cross-sectional area of one fiber;

n_X is the number of reinforcing fibers parallel to the x-axis, perpendicular to the width b of the cross-section.

Accordingly, the total cross-sectional area of the reinforcing fibers oriented along the y-axis, perpendicular to the width a of the cross-section of the reinforcing layer normal to the y-axis, is

$$A_{ay} = n_y \ A_f, \quad (9)$$

where n_y is the number of reinforcing fibers parallel to the y-axis per width a of the cross section.

We replace separately located reinforcing fibers (Figure 3b) with a solid elastic composite layer of thickness h_2 (Figure 3c) with areas of cross-sections normal to the x and y axes, respectively

$$A_{2x} = b\,h_2; \quad A_{2y} = a\,h_2, \quad (10)$$

and coefficients of reinforcement

$$\omega_x = \frac{A_{ax}}{A_{2x}}; \quad \omega_y = \frac{A_{ay}}{A_{2y}} \quad (11)$$

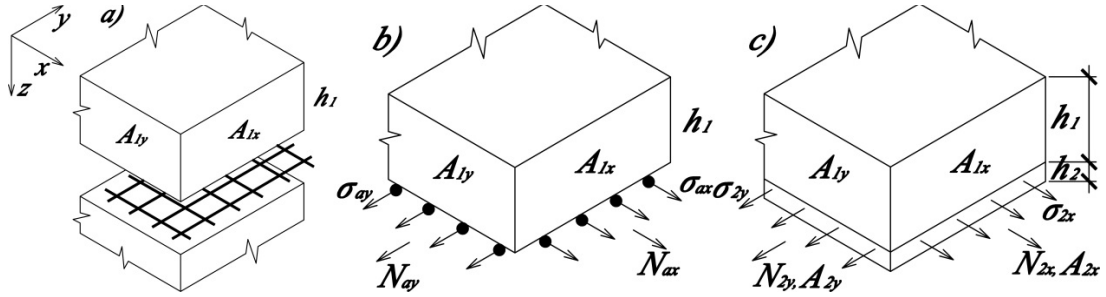

Figure 3. Reinforced plate: a) the structural scheme of a plate; b) forces and stresses in reinforcing fibers; c) forces and stresses in a continuous composite layer.

Such a replacement makes it possible to simplify and unify the design model of the reinforced layer (Figure 3a), by presenting it in the form of a two-layer system (Figure 3c) with different elastic characteristics constant within each layer.

We assume that the normal stresses σ_{2x} and σ_{2y} in a cross sections of the composite layer coinciding with the geogrid cell boundary are distributed evenly over the areas A_{2x} and A_{2y} respectively (Figure 3c) and their resultant ones are determined from the equalities

$$N_{2x} = \sigma_{2x} A_{2x}, \ N_{2y} = \sigma_{2y} A_{2y}. \quad (12)$$

The tensile forces in reinforcing fibers N_{ax} and N_{ay} represent like expressions

$$N_{ax} = \sigma_a A_{ax}, \ N_{ay} = \sigma_a A_{ay} \quad (13)$$

where σ_A is normal stress in reinforcing fiber.

Taking into account equalities (11)–(13), from conditions

$$N_{ax} = N_{2x}, \ N_{ay} = N_{2y}, \quad (14)$$

we get

$$\sigma_{2x} = \omega_x \ \sigma_a, \ \sigma_{2y} = \omega_y \ \sigma_a. \quad (15)$$

Assume that the Kirchhoff-Love hypothesis for a plate consisting of two elastic layers rigidly connected to each other is valid.

We use the Bubnov-Galerkin method [20] to calculate the multilayer plate located on an elastic base while bending. The design scheme of the plate is shown in Figure 4.

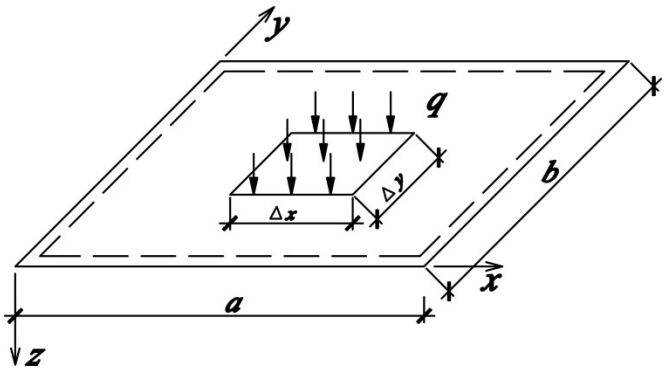

Figure 4. The design scheme of the plate located on an elastic base.

The loading area in the design scheme is taken in the rectangle form equal to area a circles tamp. The deflection function is given in the form of a double trigonometric row

$$w(x,y)=\sum_m\sum_n w_{mn}\cdot\sin\frac{m\pi x}{a}\cdot\sin\frac{n\pi y}{b} \tag{16}$$

where m and n are integers in the range 1…m and 1…n;

a and b are plate dimensions, m;

w_{mn} is the row coefficient, calculated by the formula

$$w_{mn}=\frac{q_{mn}}{(D_0+C_z)}, \tag{17}$$

here D_0 is the total plate cylindrical stiffness:

$$D_0=\left[\begin{array}{l} D_{11}\left(\frac{m\pi}{a}\right)^4+2(D_{12}+D_{33})\cdot \\ \left(\frac{m\pi}{a}\right)^2\left(\frac{n\pi}{b}\right)^2+D_{22}\left(\frac{n\pi}{b}\right)^4 \end{array}\right]; \tag{18}$$

q_{mn} is the row coefficient of load:

$$q_{mn}=\frac{16q}{\pi^2 mn}\sin\frac{m\pi}{2}\sin\frac{m\pi\Delta x}{2a}\sin\frac{n\pi}{2}\sin\frac{n\pi\Delta y}{2a} \tag{19}$$

where Δx and Δy are dimensions of loading area (Figure 4).

2.2. Experiment

Experimental studies were carried out in the form of stamp tests of two layers base of pavement structure. The upper layer consists of crushed stone fraction 40–70 mm. The layer thick h_1=0.2 m. The lower layer of thickness h_0=0.9 m is made of fine sand. The reinforcement in the form of a geogrid is located on the boundary of the layers. The reinforced base design is shown in Figure1a.

The experiment was performed in the soil channel of the Siberian State Automobile and Highway University. The soil channel has dimensions in plan of 6×3.15 m and a depth of 1.2 m.

Crushed stone was distributed layer by layer with moistening and compaction onto a previously compacted layer of sand. The total thickness of the crushed stone in the compacted state was 0.2 m. The loading was carried out through a circular rigid stamp with a diameter of 0.33 m, which simulates the imprint of the car wheel. The load was applied through a hydraulic jack in steps of 10 kN and reached 50 kN. The test setup scheme is shown in Figure 5, where B = 3.15 m.

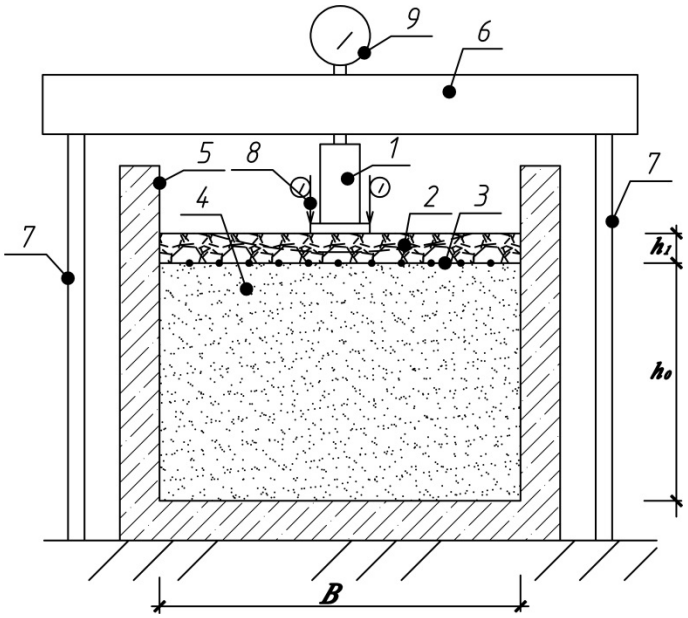

Figure 5. The test setup scheme: 1 – hydraulic cylinder of jack, 2 – crushed stone layer, 3 – geogrid, 4 – sand base, 5 – concrete tray, 6 – traverse, 7 – high rigidity rods connecting the traverse to the force floor, 8 – dial indicators with a scale value of 0,01 mm, 9 –pressure gauge of jack.

The deflections of investigated structure under the stamp were determined by the help of dial indicators with a division value of 0.01 mm mounted on the upper surface of the stamp. The indicators were attached to the reference beam to eliminate the effect of deformations of the experimental setup. The indicators rods are touched the stamp surface from opposite edges in order to eliminate the effect of a skew stamp under load (Figure 6).

**Figure 6. Photograph of large-scale model experiment set-up:
1 – hydraulic cylinder of jack, 2 – rigid stamp, 3 – dial indicators with a scale,
4 – indicator mounting rods, 5 – bench mark beams, 6 – traverse.**

The measurements were carried out both during loading and unloading the structure to select the elastic component of the deflection, which is used to calculate the modulus of elasticity. The value of the unreinforced structure deflection was determined as a control value.

The modulus of elasticity was determined from formula using the obtained values of elastic deflections [25]:

$$E_0 = \frac{Kd(1-\nu^2)\Delta q}{\Delta s}, \tag{20}$$

where K is the coefficient accepted for a rigid stamp equal of 0.79;

d is the stamp diameter, m;

ν = 0.3 is Poisson's ratio for the soil structure;

Δq is the pressure difference under the stamp, kPa;

Δs is the difference of the stamp deflections, m.

There is proposed to estimate the effect of reinforcement using the coefficient C_w, which presents the percentage between deflections of reinforced and unreinforced structure;

$$C_w = \left(1 - \frac{w_2}{w_1}\right) \cdot 100\%, \tag{21}$$

where w_1 and w_2 are the maximum deflection of unreinforced and reinforced system respectively.

The results of the tests are presented in Figure 7.

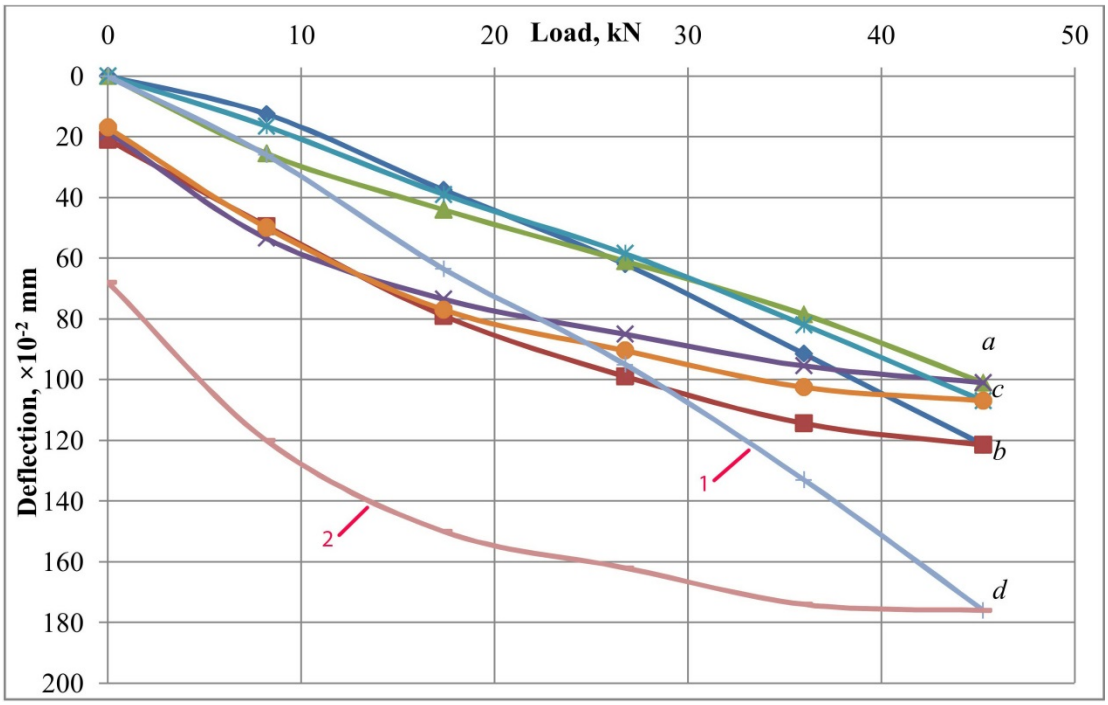

Figure 7. Load-unload diagram of reinforced (*a, b, c*) and unreinforced (*d*) structure: *a*) the number of wires inside one strip– 3; the cell size 100×100 mm; *b*) the number of wires inside one strip – 6; the cell size 75×75 mm; *c*) the number of wires inside one strip – 9: the cell size of 75×75 mm; 1) Load; 2) Unload.

According to the test results, there was a decrease in deflections for all reinforced structures. The greatest reinforcement effect was shown by a structure reinforced with a geogrid with a cell size of 100×100 mm and the number of wires inside one strip – 3. An almost linear increase in deflections is observed on the loading branches for all reinforced structures. The decrease in deflections shown on the unloading branch of the diagram occurs along a smooth curve. This type of deformation corresponds to the fact that the reinforcement of the base gives an increase in its elastic characteristics. The maximum effect of reinforcement on the deflection is 41 %, on the modulus of elasticity is 69 %.

3. Results and Discussion

An analysis of the experimental data shows that the crushed stone layer reinforcement by geogrid with steel fibers on a sandy base makes it possible to reduce the elastic deflection of the "crushed stone –sand" system by more than 40%. The results of theoretical and experimental studies are given in Table 1.

Table 1. The results of theoretical and experimental studies.

The size cells, mm	The number of reinforcing wires inside one strip	Elasticc deflection,*w*, mm		Divergences, %
		theoretical	experimental	
50×50	3	0.930	0.947	1.83
	9	0.79	0.925	17.09
75×75	3	0.950	0.860	10.47
	6	0.900	0.998	10.89
	9	0.850	0.917	7.88
100×100	3	0.970	0.862	12.53
	9	0.890	0.995	11.78

The Table 1 presents the results of theoretical and experimental studies. Their analysis and comparison shows good convergence. This is a confirmation of the adequacy of the proposed calculation model. Its essence lies in the fact that a granular layer reinforced with a geogrid can be considered as a bending plate on an elastic base. The effect of reinforcement arises due to the fact that individual grains of granular materials are grasped by the geogrid while ensuring their joint deformation.

A direct comparison of the experimental results with the results of other authors is impossible, since the geogrid with steel wires used to reinforce the bases is made relatively recently and there are no published data on the results of stamp tests of such structures in the literature. The reinforcement effect of pavement base on deflection established in this work for all sizes of geogrids with steel wires was 30–40%. A similar result (31%) was obtained when testing the construction of crushed stone bases reinforced with polymer geogrids described Mikhaylin [26].

4. Conclusions

1. A design model of a reinforced granular base of the pavement structure was created in the form of an equivalent in rigidity two-layer bending plate on an elastic base.

2. The formulas of cylindrical stiffness of a two-layer plate are received. They describe the stiffness characteristics of each of the layers and the whole package of layers.

3. The Bubnov-Galerkin variation method is used to determine the deflections of a two-layer plate. It is characterized by fast convergence.

4. The results of experimental studies in the form of a stamp test of a reinforced crushed stone base of a pavement showed a satisfactory agreement with the results of calculations by the proposed method.

The proposed calculating method for the reinforced granular base of roadbed as a two-layer plate on an elastic foundation leads to a rapidly convergent series using the technical bending theory and the Bubnov-Galerkin method. This makes it possible to apply it in practical calculations of the bases of granular materials reinforced with geogrid.

References

1. Tabatabaei, S.A., Rahman, A. The Effect of Utilization of Geogrids on Reducing the Required Thickness of Unpaved Roads [Online]. Advanced Materials Research. 2013. Vol. 712–715. Pp. 937–941. URL: https://doi.org/10.4028/www.scientific.net/AMR.712-715.937
2. Yin, J.H. Modelling Geosynthetic-Reinforced Granular Fills Over Soft Soil. Geosynthetics International. 1997. No. 4(2). Pp. 165–185.
3. Chen, Q., Hanandeh, S., Abu-Farsakh, M., Mohammad, L. Performance evaluation of full-scale geosynthetic reinforced flexible pavement [Online]. Geosynthetics International. 2018. No. 25(1). Pp. 26–36. URL: https://doi.org/10.1680/jgein.17.00031
4. Sun, X., Han, J. Mechanistic-empirical analysis of geogrid-stabilized layered systems: Part I. Solutions [Online]. Geosynthetics International. 2019. No. 26(3). Pp. 273–285. URL: https://doi.org/10.1680/jgein.19.00006
5. Sun, X., Han, J. Mechanistic-empirical analysis of geogrid-stabilized layered systems: Part II. Analysis [Online]. Geosynthetics International. 2019. No. 26(3). Pp. 286–296. URL: https://doi.org/10.1680/jgein.19.00007
6. Christopher, B., Perkins, S. Full scale testing of geogrids to evaluate junction strength requirements for reinforced roadway base design, Proceedings: The Forth European Geosynthetics Conference Eurogeo 4: Editor: Neil Dixon, Edinburg, United Kingdom, 7–10 September 2008. 8 p.
7. Chen, Q., Hanandeh, S., Abu-Farsakh, M., Mohammad, L. Performance evaluation of full-scale geosynthetic reinforced flexible pavement [Online]. Geosynthetics International. 2018. No. 25(1). Pp. 26–36. URL: https://doi.org/10.1680/jgein.17.00031
8. Tang, X., Chehab, G.R., Palomino, A. Evaluation of geogrids for stabilising weak pavement subgrade. International Journal of Pavement Engineering. 2008. Vol. 9. No. 6. Pp. 413–429. DOI: 10.1080/10298430802279827
9. Kongkitkul, W., Tabsombut, W., Jaturapitakkul, C., Tatsuoka, F. Effects of temperature on the rupture strength and elastic stiffness of geogrids. Geosynthetics International. 2012. No. 19(2). Pp. 106–123. DOI: 10.1680/gein.2012.19.2.106 10.
10. Chantachot, T., Kongkitkul, W., Tatsuoka, F. Effects of temperature rise on load-strain-time behaviour of geogrids and simulations [Online]. Geosynthetics International. 2018. No. 25(3). Pp. 287–303. URL: https://doi.org/10.1680/jgein.18.00008
11. Cardile, G., Moraci, N., Pisano, M. Tensile behaviour of an HDPE geogrid under cyclic loading: experimental results and empirical modeling [Online]. Geosynthetics International. 2016. No. 24(1). Pp. 95–112. URL: https://doi.org/10.1680/jgein.16.00019

12. Bathurst, R.J., Ezzein, F.M. Geogrid pullout load–strain behaviour and modelling using a transparent granular soil [Online]. Geosynthetics International. 2016. No. 23(4). Pp. 271–286. URL: https://doi.org/10.1680/jgein.15.00051
13. Liu, F.-Y., Wang, P., Geng, X., Wang, J., Lin, X. Cyclic and post-cyclic behaviour from sand–geogrid interface large-scale direct shear tests [Online]. Geosynthetics International. 2016. No. 23(2). Pp. 129–139. URL: https://doi.org/10.1680/jgein.15.00037
14. Ziegler, M. Application of geogrid reinforced constructions: history, recent and future developments. Procedia Engineering. 2017. No. 172. Pp. 42–51. DOI: 10.1016/j.proeng.2017.02.015
15. Ferellec, J.-F., McDowel, G.R. Modelling of ballast–geogrid interaction using the discrete-element method [Online]. Geosynthetics International. 2012. No. 19(6). Pp. 470–479. URL: https://doi.org/10.1680/gein.12.00031
16. Blanc, M., Thorel, L., Girout, R., Almeida, M. Geosynthetic reinforcement of a granular load transfer platform above rigid inclusions: comparison between centrifuge testing and analytical modeling [Online]. Geosynthetics International. 2014. No. 21(1). Pp. 37–52. URL: http://dx.doi.org/10.1680/gein.13.00033
17. Abu-Farsakh, M.Y., Chen, Q. Evaluation of geogrid base reinforcement in flexible pavement using cyclic plate load testing [Online]. International Journal of Pavement Engineering. 2011. Vol. 12, No. 3. Pp. 275–288. URL: https://doi.org/10.1080/10298436.2010.549565
18. Aleksandrov, A.S., Kalinin, A.L., Tsyguleva, M.V. Distribution capacity of sandy soils reinforced with geosynthetics. Magazine of Civil Engineering. 2016. No. 6. Pp. 35–48. DOI: 10.5862/MCE.66.4
19. Haas, R., Walls, J., Carroll, R.G. Geogrid reinforcement of granular bases in flexible pavements. Transportation Research Record. 1988. No. 1188. Pp. 19–27.
20. Matveev, S.A., Martynov, E.A., Litvinov, N.N. Eksperimental'no-teoreticheskiye issledovaniya armirovannogo osnovaniya dorozhnoy odezhdy [Experimental and theoretical studies of the reinforced base of the pavement] [Online]. Vestnik SIBADI. 2015. No. 4(44). Pp. 77–83. URL: https://doi.org/10.26518/2071-7296-2015-4(44)-80-86. (rus)
21. Matveev, S.A., Martynov, E.A., Litvinov, N.N. Effect of Reinforcing The Base of Pavement With Steel Geogrid [Online]. Applied Mechanics and Materials. 2014. Vol. 587–589. Pp. 1137–1140. URL: https://doi.org/10.4028/www.scientific.net/AMM.587-589.1137
22. Matveev, S.A., Martynov, E.A., Litvinov, N.N. Determine The Reinforcement Effect of Gravel Layer on a Sandy Foundation [Online]. Applied Mechanics and Materials. 2014. Vol. 662. Pp. 164–167. URL: https://doi.org/10.4028/www.scientific.net/AMM.662.164
23. Rakowski, Z. An attempt of the synthesis of recent knowledge about mechanisms involved in stabilization function of geogrids in infrastructure constructions [Online]. Procedia Engineering. 2017. No. 189. Pp. 166–173. URL: https://doi.org/10.1007/978-3-030-01908-2_14
24. Berestyanii, Y.B., Valtseva, T.U., Mikhailin, R.G., Goncharova E.D. Motorway Structures Reinforced with Geosynthetic Materials in Polar Regions of Russia. The 24rd International Offshore (Ocean) and Polar Engineering Conference. Bussan, Korea. 2014. Pp. 502–506.
25. State standard GOST 20276-2012. Soils. Methods of field determination of durability and deformability's characteristics. Moscow, 2013. 32 p. (rus)
26. Mikhaylin, R.G. Sovershenstvovanie metodiki rascheta armirovaniya nezhestkix dorozhny`x odezhd georeshetkami [The improving of methodology for calculating of flexible pavement reinforcement with geogrids]: PhD Diss: 05.23.11. Khabarovsk, 2016. 114 p. (rus)

Contacts:

Sergey Matveev, dfsibadi@mail.ru
Evgeny Martynov, asp_evg@mail.ru
Nikolai Litvinov, niklitvinov_23@mail.ru
Grigoriy Kadisov, kadisov@rambler.ru
Vladimir Utkin, prof.utkin@mail.ru